AGU PUBLICATIONS

Geophysical Research Letters

RESEARCH LETTER
10.1002/2016GL071055

Key Points:
- The seasonal cycle in TOA radiation provides a constraint on observational estimates of planetary heat content
- The seasonal cycle in ocean heat content of regions with limited Argo data is poorly estimated by the average across measured regions
- The lack of spatially complete measurements of upper ocean temperature may lead to an underestimation of the magnitude of planetary heating

Supporting Information:
- Supporting Information S1
- Figure S1

Correspondence to:
K. A. McKinnon,
mckinnon@ucar.edu

Citation:
McKinnon, K. A., and P. Huybers (2016), Seasonal constraints on inferred planetary heat content, *Geophys. Res. Lett.*, *43*, 10,955–10,964, doi:10.1002/2016GL071055.

Received 31 AUG 2016
Accepted 13 OCT 2016
Accepted article online 18 OCT 2016
Published online 30 OCT 2016

Seasonal constraints on inferred planetary heat content

Karen A. McKinnon[1] and Peter Huybers[2]

[1]Climate and Global Change Division, National Center for Atmospheric Research, Boulder, Colorado, USA, [2]Department of Earth and Planetary Sciences, Harvard University, Cambridge, Massachusetts, USA

Abstract Planetary heating can be quantified using top of the atmosphere energy fluxes or through monitoring the heat content of the Earth system. It has been difficult, however, to compare the two methods with each other because of biases in satellite measurements and incomplete spatial coverage of ocean observations. Here we focus on the the seasonal cycle whose amplitude is large relative to satellite biases and observational errors. The seasonal budget can be closed through inferring contributions from high-latitude oceans and marginal seas using the covariance structure of National Center for Atmospheric Research (NCAR) Community Earth System Model (CESM1). In contrast, if these regions are approximated as the average across well-observed regions, the amplitude of the seasonal cycle is overestimated relative to satellite constraints. Analysis of the same CESM1 simulation indicates that complete measurement of the upper ocean would increase the magnitude and precision of interannual trend estimates in ocean heating more than fully measuring the deep ocean.

1. Introduction

Knowledge of the energy imbalance of the planet is critical for the quantification of climate sensitivity, climate model validation, and improved predictions of future warming [*von Schuckmann et al.*, 2016]. Earth's energy imbalance can be inferred through measuring net radiation at the top of the atmosphere (TOA) or monitoring changes in the heat content of the oceans and other elements of the Earth system. Ideally, these two approaches would offer the opportunity for intercomparison because heating at the TOA must lead to an increase in the heat content of the underlying Earth system, but measurement biases and uncertainties make such validation difficult.

The Clouds and the Earth's Radiant Energy System (CERES) satellite has measured net TOA radiation since March 2000 with high precision (within 0.3 Wm^{-2} per decade) [*Loeb et al.*, 2007], but the measurements are known to be biased [*Loeb et al.*, 2009] and so do not allow for estimation of the absolute TOA heating rate. Conversely, it is difficult to make spatially and temporally complete measurements of heat content, the majority of which is stored in the ocean [e.g., *Wunsch*, 2016]. Since 2000, Argo floats have improved the sampling of the ocean [e.g., *Abraham et al.*, 2013], but there remain potentially important measurement gaps in the deep ocean, some marginal seas, and at high latitudes [*von Schuckmann et al.*, 2016].

Due to the large bias of the CERES measurements and the sparsity of the Argo measurements compared to the volume of the ocean, researchers have combined the best components of each—the precision of CERES and the mean value from Argo—to obtain better estimates of the TOA energy imbalance over time [e.g., *Loeb et al.*, 2012; *Johnson et al.*, 2016]. Satellite measurements, in situ data, and atmospheric reanalyses have also been used to constrain dynamical ocean models in order to improve estimates of heat content and other ocean properties [e.g., *Wunsch and Heimbach*, 2013; *Balmaseda et al.*, 2013; *Zuo et al.*, 2015]. Such combined estimates have obvious advantages but do not permit for verification across independent methods and data sets.

The agreement between in situ ocean measurements and TOA radiation has been assessed for interannual variability [*Loeb et al.*, 2012; *Trenberth et al.*, 2016; *Johnson et al.*, 2016], which is less affected than trend calculations by biases in CERES measurements, but the signal is difficult to identify because the magnitude of interannual variability is comparable to the uncertainty in estimates of ocean heat content.

In contrast, the seasonal cycle is a repeated signal that is larger than uncertainties in ocean heat content. Furthermore, estimates of the amplitude and phase of the seasonal cycle in heating measured by CERES are not susceptible to issues of bias in absolute magnitudes that confound estimates of interannual trends.

As such, one can independently compare ground and satellite estimates. This comparison demonstrates challenges in closing the planetary energy budget using Argo measurements and suggests the importance of continuing to expand ocean measurements to the high latitudes and marginal seas.

2. Data

Analysis focuses on the years 2005–2014, spanning the era during which both CERES and Argo data are available, excluding the first 5 years of Argo when float coverage was rapidly increasing. While using such a short time period can be problematic for estimating trends, it contains 10 iterations of the seasonal cycle and therefore allows for a relatively stable estimate of the seasonality of planetary heat content. TOA radiation measurements are from the CERES satellite [*Wielicki et al.*, 1996]. We use the SYN1deg product that, unlike EBAF-TOA, is available at daily resolution and does not use the global average heating rate estimated from Argo data [*Loeb et al.*, 2009].

Our primary source of ocean temperature measurements is the widely used Scripps gridded product [*Roemmich and Gilson*, 2009]. The product is created through optimal interpolation of Argo trajectories. The trajectories are gridded to $1^\circ \times 1^\circ$ in the horizontal in a domain (hereafter the Scripps domain, called the OI domain in *Roemmich et al.* [2015]) that spans 60°S–60°N and excludes the marginal seas (Figure 1). Argo floats do not measure the ocean below 2000 m, although there are efforts underway to deploy floats capable of monitoring such depths (Deep Argo) [*Johnson et al.*, 2015]. The Scripps domain is thus lacking coverage of 56% of the total ocean volume and 9.5% of the upper 2000 m. Among the unmapped regions of the upper ocean, two thirds of the volume is in the high latitudes and one third is in the marginal seas.

The Scripps product appears to uniquely provide monthly data that only incorporates information from Argo floats, including that the baseline climatology is itself estimated from Argo measurements. The seasonal cycle in the Scripps product can thus be used to explore the precision and accuracy of Argo-based ocean heat content estimates. Other direct and indirect sources of information for ocean temperature and heat content do exist, such as instrumented sea mammals [*Roquet et al.*, 2013], ice-tethered buoys [*Toole et al.*, 2011], sea surface temperatures [e.g., *Ishii and Kimoto*, 2009], sea surface height [e.g., *Willis et al.*, 2004; *Johnson et al.*, 2013; *von Schuckmann et al.*, 2014], and reanalyses [e.g., *Zuo et al.*, 2015]. However, motivated by the fact that Argo data are currently the largest source of subsurface temperature data and recent estimates of ocean heat content trends have often relied solely on Argo data [e.g., *Lyman et al.*, 2010; *von Schuckmann and Traon*, 2011; *von Schuckmann et al.*, 2013; *Roemmich et al.*, 2015; *Wijffels et al.*, 2016], our ocean analysis also focuses exclusively on Argo data.

Energy is also seasonally stored in the atmosphere, land, and cryosphere. Although these reservoirs account for only a small part of the multiyear trend in heat content [*Abraham et al.*, 2013], they have a nontrivial seasonal cycle. The vertically integrated total energy content of the atmosphere—including sensible, latent, potential, and kinetic energy—is based on the ERA-interim reanalysis [*Dee et al.*, 2011] and is calculated using the methods of *Trenberth et al.* [2001]. The heat content of the land surface is estimated using climatological surface temperature data from Berkeley Earth [*Rohde et al.*, 2013] combined with a representation of heat conduction into the solid Earth following the approach of *Hansen et al.* [2011]. Arctic sea ice volume is calculated using the Pan-Arctic Ice Ocean Modeling and Assimilation System (PIOMAS) [*Zhang and Rothrock*, 2003], and Antarctic sea ice extent is based upon satellite passive microwave data [*Fetterer and Knowles*, 2004]. Antarctic sea ice volume information is not available, so we assume a constant ice thickness of 0.9 m [*Worby et al.*, 2008]. The seasonal cycles of heat content associated with land ice variations [*Jacob et al.*, 2012] and snow [*Robinson et al.*, 1993; *Willmott et al.*, 1985] are at least an order of magnitude less than the other components and are neglected. See Table S1 in the supporting information for the physical parameters assumed when estimating the energy stored in these reservoirs.

The focus of this work is on estimating the planetary heat content from integrated TOA radiation and ground-based measurements of heat content, but two other approaches are of note. One is to integrate net energy fluxes at the surface but which is confounded by the sparsity of direct flux observations and the large global imbalances within atmospheric reanalyses [*von Schuckmann et al.*, 2016]. The other is to quantify planetary heating through coupled model simulations that conserve energy [e.g., *Smith et al.*, 2015; *Wild et al.*, 2015], but there remain major questions regarding model bias and representations of external radiative forcing. An expanded analysis of the seasonal cycle of planetary heating based on these approaches may be useful in future work.

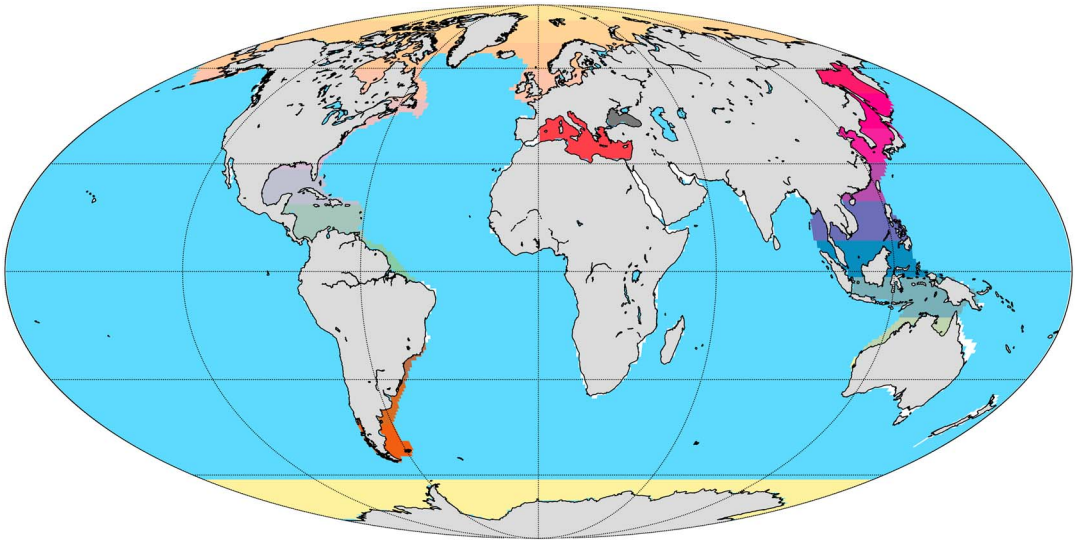

Figure 1. Scripps domain. Light blue regions indicate gridboxes with temperature profile estimates down to 2000 m based upon optimal interpolation (OI) of Argo data from *Roemmich and Gilson* [2009], termed the Scripps domain in text. The colored and white regions indicate gridboxes not infilled through OI due to limited measurements. Unfilled gridboxes are grouped into contiguous regions for infilling using the covariance structure of CESM1 (see Text S1). The 25 largest contiguous regions are indicated in colors. The remaining regions are not distinguished from each other in the figure for clarity and are all colored white.

3. The Seasonal Cycle in Heat Content

The seasonal cycle in heat content can be precisely estimated from CERES. Daily average measurements of radiation are converted to anomalous heat content values at each gridbox through removing the sample mean across the full time series, after which they are integrated across time and the surface area of the Earth. Surface area is estimated assuming a spherical planet with a radius of 6371.220 km, and results are reported at monthly resolution. The integration yields a climatological seasonal cycle in planetary heat content that has an amplitude of 22 ZJ (1 ZJ = 10^{21} J), measured as half the difference between the monthly maximum and minimum of the climatology.

The seasonal cycle deviates slightly from a sinusoid in that planetary heat content decreases more quickly from boreal spring to autumn than it increases from boreal autumn to spring. The peak of the seasonal cycle of heat content occurs in April, at the end of the Southern Hemisphere summer, consistent with its greater ocean volume. The standard deviation of monthly anomalies around the climatology averages 1.6 ZJ across months or an order of magnitude smaller than the amplitude of the seasonal cycle.

For comparison with the satellite-based estimates, the heat content of the atmosphere, land, cryosphere, and ocean are combined. Among the nonocean components of the budget, the atmosphere has the greatest amplitude at 8.1 ZJ. The maxima of atmospheric energy content occur in July, shortly after Northern Hemisphere summer solstice, consistent with a small atmospheric heat capacity and greater land mass of the Northern Hemisphere that both heats and provides moisture to the atmosphere (Figure 2a). The seasonal cycle of land heat content has an amplitude of 4.2 ZJ and peaks in September, again reflecting greater Northern Hemisphere land mass. The seasonal cycle of cryospheric heat content is dominated by sea ice variability and has two maxima during the year, in March and October, because of different phasing of the Arctic and Antarctic. Uncertainty in each component of the heat budget is estimated as the spread of individual years around the 10 year climatology, and uncertainties in their sum are estimated analogously.

The majority of the seasonal cycle in planetary heat content is comprised of variations in ocean heat storage (Figure 2a). Because Argo floats provide only sparse measurements in the highest latitudes, some marginal seas, and the deep ocean, estimates of planetary heat content using Argo data require implicit or explicit assumptions regarding the relationship between the heat content of the measured and unmeasured regions. We focus on the influence of infilling assumptions for the umapped high latitudes and marginal seas in the Scripps domain. The seasonal cycle cannot be used to examine assumptions about the deep ocean because

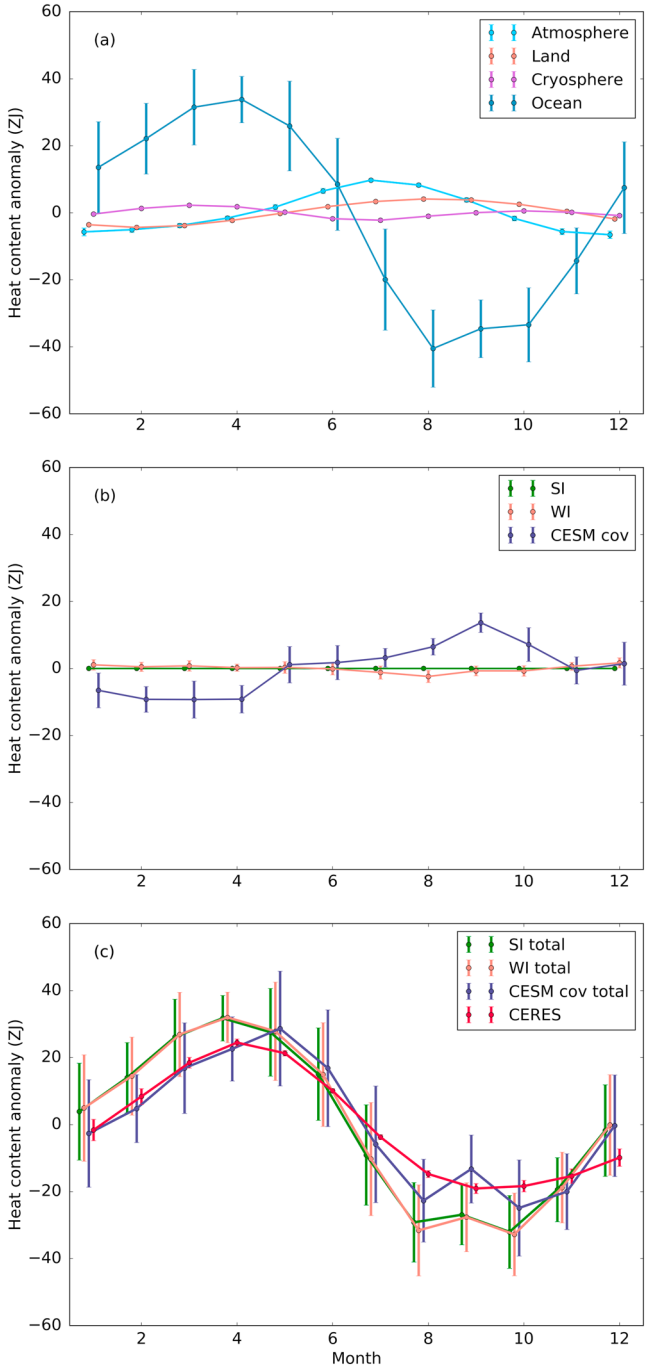

Figure 2. The seasonal cycle of planetary heat content. (a) The seasonal cycle of each component of planetary heat content. The ocean component is from the Scripps domain only. The vertical bars show one standard deviation of the year-to-year variability for each month, and the dots indicate the mean value across all years. The year-to-year variability for the land, atmosphere, and cryosphere is small on the scale of the plot. (b) The seasonal cycle of heat content estimated for the regions lacking data in the Scripps product using different infilling methods. (c) The seasonal cycle in planetary heat content calculated from CERES measurements (red) as compared to estimates using the Simple Integral (green), Weighted Integral (yellow), and CESM1 covariance (purple) infilling methods.

of its shallow vertical penetration. Whereas there are a range of methods in the literature for estimating the global integral of heat content from spatially incomplete data, we examine the effect of two commonly used assumptions termed the "Simple Integral" (SI) and "Weighted Integral" (WI) by *Lyman and Johnson* [2008] that have been used in many prior studies (e.g., *Levitus et al.* [2005], *Ishii et al.* [2006], and *Levitus et al.* [2012] for SI and *Palmer et al.* [2007], *Lyman et al.* [2010], *Roemmich et al.* [2015], and *Cheng and Zhu* [2015] for WI).

The underlying assumption for the SI method is that the global integral can be calculated as the integral over the available data or that the mean of the anomaly field in the unobserved regions is zero. In contrast, the WI approach assumes that the observed regions are representative of the unobserved regions. Here we evaluate the seasonality implied by both methods. The SI-based estimate of heat content is calculated by assuming the anomalies in the high latitudes and marginal seas are zero. Due to the opposite phasing of the seasonal cycles across hemispheres, we calculate the WI-based estimate by infilling missing regions with either the relevant extratropical or tropical (23°S–23°N) volume-weighted average value. Other approaches, such as using smaller regions as representative averages [*von Schuckmann and Traon*, 2011; *Gouretski et al.*, 2012] or using information from sea surface height to infill missing data [*Willis et al.*, 2004; *Domingues et al.*, 2008; *Johnson et al.*, 2013], are not considered here.

The amplitude of the seasonal cycle in oceanic heat content in the Scripps domain is 37 ZJ (Figure 2a). By construction, the SI approach yields the same value. The WI approach leads to a small increase in the amplitude to 38 ZJ because a larger volume of the Southern Hemisphere extratropical ocean is infilled than in the Northern Hemisphere, and the seasonal cycle in planetary heat content is in phase with Southern Hemisphere heat content. However, the increase is small because the amplitude of the seasonal cycle in heat content per unit volume in the measured regions is larger in the Northern than Southern Hemisphere (Figure 2b). The resulting estimates are combined with the nonocean terms in the heat budget in order to assess closure with respect to the CERES data. In both cases, the inferred planetary heat content has a seasonal cycle that has too large an amplitude compared to the CERES measurements (Figure 2c).

The misfit using both approaches is primarily due to the lack of measurements in the high latitude Northern Hemisphere waters where the seasonal cycle of heat content has a large amplitude and is of opposite phase to the seasonal cycle of the planetary heat budget. The lack of closure is quantified through an examination of the residuals between the CERES-based and infilled estimates. In particular, if the two estimates were consistent, the residuals should not have seasonal structure, which we quantify using the autocorrelation of the residuals at a lag of 12 months. The lag-12 autocorrelation of the SI-based (WI-based) residuals is 0.25 (0.24) for the Scripps data set, which is greater than that expected from Gaussian white noise at the 0.01 level. The distribution of autocorrelations from white noise is calculated using the complementary inverse error function.

Another potential method for creating a gridded product from Argo float data is Kriging. We opt not to pursue this approach, however, because the spatial scales of monthly heat content anomalies within Argo [e.g., *Roemmich and Gilson*, 2009, Figure 2.2] are small compared to the distance between regions that are consistently sampled and sparsely sampled by Argo floats. This leads to uncertainties in the mapping that are larger than the signal, especially in the extratropics. More fundamentally, Kriging assumes stationary statistical properties across the domain [e.g., *Cressie*, 1993]. From 2005 to 2014, Argo floats have been less likely to measure high-latitude oceans and some marginal seas. These regions are influenced by factors such as the formation of sea ice and bathymetric contraints that are not present in the open ocean.

Instead, we take advantage of a fully coupled dynamical model, National Center for Atmospheric Research (NCAR) Community Earth System Model (CESM1) [*Hurrell et al.*, 2013], to provide information about the covariance structure between the mapped and unmapped parts of the ocean, analogous to the approach of *Cheng and Zhu* [2016] using Coupled Model Intercomparison Project Phase 5 (CMIP5) simulations. The assumption underlying the infilling method is not that CESM1 is properly representing the actual seasonal cycle in heat content, but rather that it can reproduce the correct spatial covariance structure on seasonal timescales. See Text S1 for details of the methodology.

The estimated seasonal cycle of heat content in the regions without Scripps data based on the CESM1 covariance structure is in phase with Northern Hemisphere heat content and therefore of opposite phase from the global average seasonal cycle of planetary heat content (Figure 2b). The phasing results from a larger amplitude of seasonal heat storage per unit volume in the Northern Hemisphere than in the Southern Hemisphere,

and this effect dominates over the greater Southern Hemisphere ocean volume, unlike in the WI approach. Combining heat content from the infilled and observed regions yields a seasonal cycle of planetary heat content of smaller amplitude that is visually consistent with the CERES data (Figure 2c). The residuals between the two estimates have a lag-12 month autocorrelation of 0.11, consistent with white noise (p value = 0.2).

Given the high precision and minimal interannual variability of the TOA radiation measurements of planetary heat content, we infer that the monthly misfits between the satellite- and ground-based estimates are primarily indicative of uncertainties from measurement and infilling in the ground-based calculation of heat content. The standard deviation of the residuals varies from a minimum of 9.7 ZJ in February to a maximum of 18 ZJ in May. Uncertainty is largest during Southern Hemisphere winter (May through July). Across all months and years, the standard deviation of the residuals is 15 ZJ. Note that this estimate of error does not account for uncertainty in the annual mean value of heat content.

Our focus thus far has been on inferences possible using the Scripps Argo-only gridded product. We also briefly assess seasonal closure with two other products that provide spatially complete estimates of subsurface ocean temperatures: the Met Office EN4 data set [*Good et al.*, 2013] and the World Ocean Atlas (WOA13) [*Locarnini et al.*, 2013]. Both data sets are produced from optimal interpolation but differ from the Scripps data set in that they incorporate non-Argo data and that their baseline climatologies are estimated from multiple decades of observations, to which undersampled regions relax toward. Because WOA13 provides a monthly climatology rather than monthly data, we use the climatology based on observations from 2005–2012 for the closest comparison to the analysis of the Scripps product.

The seasonal cycle in planetary heat content using EN4 data is consistent with satellite constraints within uncertainty, although the best estimate of its amplitude (17 ZJ) is smaller than that of the satellite data (22 ZJ). Uncertainties in the WOA13 climatology cannot be estimated as with the other products because the interannual variability of the monthly values is not available; if the monthly uncertainty around the climatology is assumed to be the same as EN4, the estimates of the seasonal budget are also found to be consistent with satellite constraints. The result suggests that the ocean has been sampled sufficiently well and has been sufficiently stable over the latter half of the twentieth century that the climatology in ocean heat content can be relatively well estimated. This level of data coverage, however, is not available on the year-to-year basis required for estimation of trends, so the closure on seasonal timescales does not necessarily suggest closure with respect to interannual trends. In section 4, we thus return to our analysis of the impact of incomplete sampling on interannual trends in the context of the data availability in the Scripps domain.

4. Importance of Marginal and High-Latitude Seas for Interannual Heating Trends

The analysis of the seasonal cycle highlights the important role of marginal and high-latitude seas for the seasonal planetary heat budget. We now turn our attention to the effects of incomplete sampling on estimates of interannual *trends* in heat content. The seasonal cycle is not expected to serve as an exact analog for trends due to its shallow nature, differences in covariance structures, and the presence of interannual persistence in heat content anomalies not accounted for in the seasonal analysis. Nonetheless, the challenges of closing the seasonal budget using common infilling assumptions raise the possibility that the same methods may also be unsuccessful for trends. Our trend analysis is performed entirely within the context of the CESM1 simulation also used in the prior section so that the accuracy of trend estimates made using different sampling strategies can be quantified.

We first confirm that CESM1 behaves similarly to the observations with regard to the seasonal infilling methods (Figure 3a). When masked to the Scripps domain, the seasonal cycle in ocean heat content is overestimated, and the overestimation is exacerbated using the WI infilling method. Infilling the masked regions based on the CESM1 covariance structure produces estimates of seasonal amplitude that are consistent with the values calculated using the full upper ocean, which is unsurprising given that for this check the analysis is self-contained within CESM1. As expected, the amplitude of the seasonal cycle with and without the deep ocean included is very similar.

The trend in ocean heat content between 2005 and 2014 is calculated using least squares regression on the monthly CESM1 output after the seasonal climatology has been removed. The trend in CESM1 heat content across the full ocean is 0.58 W m^{-2} (Figure 3b). While 0.056 W m^{-2} of the heating accumulated in the deep

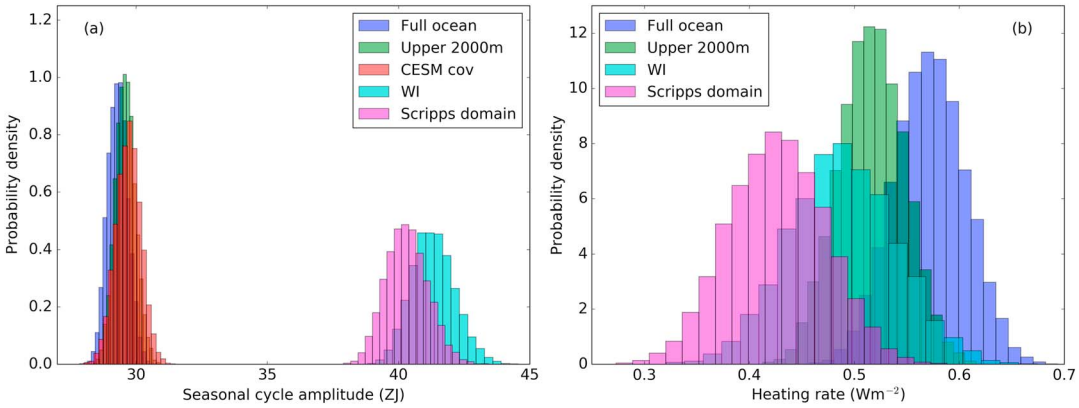

Figure 3. The seasonal cycle and trends in ocean heat content within CESM1 for 2005–2014. (a) The amplitude of the seasonal cycle based upon different masking and infilling strategies. The distributions are estimated through resampling years with replacement 10,000 times before calculating the climatology. (b) Trends in ocean heat content based upon different masking and infilling strategies. Distributions are calculated through the use of a block bootstrap (see main text).

ocean below 2000 m, a total of 0.091 W m^{-2} accumulated in the high latitudes (0.077 W m^{-2}) and marginal seas (0.014 W m^{-2}), despite the fact that these regions only cover 9.5% of the volume of the upper 2000 m of the ocean.

We do not attempt to infer the magnitude of heating in the high latitudes and marginal seas in the Scripps product through infilling via the covariance in CESM1, as was done for the seasonal cycle, because we find that neither the seasonal nor interannual covariance structure can skillfully predict decadal trends even within CESM1. We do, however, calculate the inferred heating rate using the WI approach implemented within CESM1, which leads to an estimate of upper ocean heating of 0.49 W m^{-2} as compared to the true value of 0.52 W m^{-2}. This underestimation occurs because high-latitude oceans cover 7% of the volume but account for 14% of the warming of the upper ocean. Of this heat, 60% is in the high northern latitudes and 40% is in the high southern latitudes. The situation is analogous to inferences that global surface temperature trends are biased low through assuming Arctic warming rates are proportional to observed regions [cf. *Cowtan and Way*, 2014]. The marginal seas cover 3% of the volume and account for a proportional 3% of the warming.

We next examine the uncertainty in estimating the planetary heating rate due to internal variability around the linear trend. The uncertainty is estimated by first removing the best fit trend from the data, performing a block bootstrap on the residuals using a block size of 1 year, adding the best fit trend back to the bootstrapped residuals, and then reestimating the trend (Figure 3b). The standard deviation of the distribution resulting from iterating the foregoing procedure 10,000 times is used as a metric for trend uncertainty. Uncertainties are similar for the heating rate of the full ocean and only the upper 2000 m of the ocean at 0.033 W m^{-2} and 0.032 W m^{-2}, respectively.

In contrast, a lack of measurements in the marginal seas and high latitudes leads to a 47% increase in the standard deviation of the distribution of heating rates (0.046 W m^{-2}) compared to the case in which the upper ocean is fully sampled. Increased uncertainty is due to a negative correlation ($r = -0.79$) in the interannual variability of anomalous heat content in CESM1 between the regions with and without upper ocean data in the Scripps domain, perhaps due to oceanic heat transport or shifting of fronts. It follows that using the WI approach further increases the uncertainty in the trends to 0.051 W m^{-2} because the method enforces positive interannual covariance between the mapped and unmapped regions — the opposite of what is present in the model. These results indicate that taking measurements in the high latitudes and marginal seas is important for both the precision and accuracy of estimates of oceanic heating rates.

5. Discussion and Conclusion

The magnitude of Earth's energy imbalance is one of the most important quantities with respect to understanding climate change [*Trenberth*, 2009; *von Schuckmann et al.*, 2016]. Although measurements of the ocean have improved dramatically in terms of spatial extent and quality in the Argo era, it is not yet clear whether

the currently available measurements allow for closure of the planetary energy budget. We focused primarily on the seasonal cycle because high-precision satellite measurements of TOA radiation provide a strong constraint on its amplitude and phase. The seasonal analysis demonstrates that not accounting for the contribution of the high latitudes and marginal seas leads to overestimation of the seasonal amplitude of planetary heat content and that this bias is not remedied through assuming that these unmapped regions of the ocean can be represented by averages across the mapped regions.

Examination of the seasonal cycle in planetary heat content has two implications for interannual heating rates. First, interannual heating rate estimates are sensitive to the choice of ocean heat content climatology when sampling is spatially incomplete [*Lyman and Johnson*, 2014; *Cheng and Zhu*, 2015; *Boyer et al.*, 2016]. Given the satellite constraint on the seasonal budget, it may be advantageous to determine whether a chosen climatology is consistent with satellite data before using it as the baseline for trend analyses.

Second, our seasonal analysis suggests caution when making assumptions regarding the heat content of unmapped regions. Within CESM1, the volume-weighted ocean heat content has increased faster from 2005 to 2014 in the high latitudes than in the Scripps domain. If these simulated trends hold in reality, prior estimates of oceanic heating using either the SI or WI approach for infilling [e.g., *Levitus et al.*, 2005; *Ishii et al.*, 2006; *Levitus et al.*, 2012; *Palmer et al.*, 2007; *Lyman et al.*, 2010; *Roemmich et al.*, 2015; *Cheng and Zhu*, 2015] may be underestimates. This possibility is consistent with recent results that find larger planetary heating rates when sea surface heights [*Durack et al.*, 2014] or data-constrained ocean models [*Trenberth et al.*, 2016] are instead used to infer heat content in regions with limited Argo measurements, and analogous to the finding that the addition of Argo to the ocean observing network led to an increase in estimated ocean heating [*Cheng and Zhu*, 2014]. Incomplete spatial coverage also increases month-to-month variability in the global integral of heat content within CESM1 because of a negative covariance between the heat content of mapped and unmapped regions. This negative covariance likely contributes to the fact that Argo-based estimates of Earth's energy imbalance have considerably more monthly variability than either TOA radiation or ocean reanalyses [*Trenberth et al.*, 2016].

The seasonal heat budget can be closed through combining the covariance structure in CESM1 with observations; however, this method was not applicable for interannual trends on account of the covariance structure diagnosed within CESM1 not being generalizable to interannual timescales. Choice of mapping technique is identified as the greatest source of uncertainty in interannual trends in ocean heat content [*Boyer et al.*, 2016], and it would be useful to systematically assess their skill on seasonal timescales. Demonstration of seasonal closure would arguably be a useful benchmark, although differences between seasonal and interannual covariance structures, especially as they relate to the vertical penetration of the seasonal cycle, suggest it would only be a partial test of accuracy in estimating interannual trends. These results underscore that more complete observation of the ocean would be the most assured method of accurately determining Earth's radiative imbalance.

Acknowledgments

The authors thank Kevin Trenberth, Carl Wunsch, and two anonymous reviewers for their helpful comments. While this article was in press, the authors were made aware that Aaron Donohoe has presented similar results that are as yet unpublished. K.A.M. acknowledges NASA NESSF and the NCAR Advanced Study Program for funding. P.J.H. acknowledges NSF grant 1304309. Gridded Argo temperature data from Scripps are at http://www.argo.ucsd.edu/Gridded_fields.html, WOA13 data are at https://www.nodc.noaa.gov/cgi-bin/OC5/woa13/woa13.pl, Met Office EN4 data are at http://www.metoffice.gov.uk/hadobs/en4/, PIOMAS Arctic sea ice volume data are at http://psc.apl.uw.edu/wordpress/wp-content/uploads/schweiger/ice_volume/PIOMAS.2sst.monthly.Current.v2.1.txt, Antarctic sea ice extent data are at https://www.ncdc.noaa.gov/snow-and-ice/extent/sea-ice/S/0.csv, vertically integrated atmospheric heat is available at http://www.cgd.ucar.edu/cas/catalog/reanalysis/budgets/index.html, Berkeley Earth temperature data are available at http://berkeleyearth.org/data/, and CESM1 monthly ocean temperature output is available at https://www.earthsystemgrid.org/dataset/ucar.cgd.ccsm4.CESM_CAM5_BGC_LE.ocn.proc.monthly_ave.html. All codes necessary for the analysis are publicly available at https://github.com/karenamckinnon/seasonal-ohc.

References

Abraham, J., et al. (2013), A review of global ocean temperature observations: Implications for ocean heat content estimates and climate change, *Rev. Geophys.*, *51*, 450–483, doi:10.1002/rog.20022.

Balmaseda, M. A., K. E. Trenberth, and E. Källén (2013), Distinctive climate signals in reanalysis of global ocean heat content, *Geophys. Res. Lett.*, *40*, 1754–1759, doi:10.1002/grl.50382.

Boyer, T., et al. (2016), Sensitivity of global upper ocean heat content estimates to mapping methods, XBT bias corrections, and baseline climatologies, *J. Clim.*, *29*, 4817–4842.

Cheng, L., and J. Zhu (2014), Artifacts in variations of ocean heat content induced by the observation system changes, *Geophys. Res. Lett.*, *41*, 7276–7283, doi:10.1002/2014GL061881.

Cheng, L., and J. Zhu (2015), Influences of the choice of climatology on ocean heat content estimation, *J. Atmos. Oceanic Technol.*, *32*(2), 388–394.

Cheng, L., and J. Zhu (2016), Benefits of CMIP5 multimodel ensemble in reconstructing historical ocean subsurface temperature variations, *J. Clim.*, *29*, 5393–5416, doi:10.1175/JCLI-D-15-0730.1.

Cowtan, K., and R. G. Way (2014), Coverage bias in the HadCRUT4 temperature series and its impact on recent temperature trends, *Q. J. R. Meteorol. Soc.*, *140*(683), 1935–1944.

Cressie, N. (1993), *Statistics for Spatial Data: Wiley Series in Probability and Statistics*, vol. 15, 16 pp., Wiley-Interscience, New York.

Dee, D., et al. (2011), The ERA-Interim reanalysis: Configuration and performance of the data assimilation system, *Q. J. R. Meteorol. Soc.*, *137*(656), 553–597.

Domingues, C. M., J. A. Church, N. J. White, P. J. Gleckler, S. E. Wijffels, P. M. Barker, and J. R. Dunn (2008), Improved estimates of upper-ocean warming and multi-decadal sea-level rise, *Nature*, *453*(7198), 1090–1093.

Durack, P. J., P. J. Gleckler, F. W. Landerer, and K. E. Taylor (2014), Quantifying underestimates of long-term upper-ocean warming, *Nat. Clim. Change*, *4*(11), 999–1005.

Fetterer, F., and K. Knowles (2004), Sea ice index monitors polar ice extent, *Eos Trans. AGU*, *85*(16), 163–163.

Good, S. A., M. J. Martin, and N. A. Rayner (2013), EN4: Quality controlled ocean temperature and salinity profiles and monthly objective analyses with uncertainty estimates, *J. Geophys. Res. Oceans*, *118*, 6704–6716, doi:10.1002/2013JC009067.
Gouretski, V., J. Kennedy, T. Boyer, and A. Köhl (2012), Consistent near-surface ocean warming since 1900 in two largely independent observing networks, *Geophys. Res. Lett.*, *39*, L19606, doi:10.1029/2012GL052975.
Hansen, J., M. Sato, P. Kharecha, and K. von Schuckmann (2011), Earth's energy imbalance and implications, *Atmos. Chem. Phys.*, *11*(24), 13,421–13,449.
Hurrell, J. W., M. Holland, P. Gent, S. Ghan, J. Kay, P. Kushner, J.-F. Lamarque, W. Large, D. Lawrence, and K. Lindsay (2013), The community Earth system model: A framework for collaborative research, *Bull. Am. Meteorol. Soc.*, *94*, 1339–1360.
Ishii, M., and M. Kimoto (2009), Reevaluation of historical ocean heat content variations with time-varying XBT and MBT depth bias corrections, *J. Oceanogr.*, *65*(3), 287–299.
Ishii, M., M. Kimoto, K. Sakamoto, and S.-I. Iwasaki (2006), Steric sea level changes estimated from historical ocean subsurface temperature and salinity analyses, *J. Oceanogr.*, *62*(2), 155–170.
Jacob, T., J. Wahr, W. T. Pfeffer, and S. Swenson (2012), Recent contributions of glaciers and ice caps to sea level rise, *Nature*, *482*(7386), 514–518.
Johnson, G., J. Lyman, J. Willis, S. Levitus, T. Boyer, J. Antonov, S. Good, C. Domingues, and N. Bindoff (2013), Ocean heat content, in *State of the Climate in 2012*, edited by J. Blunden and D. S. Arndt, *Bull. Am. Meteorol. Soc.*, S54–S60.
Johnson, G. C., J. M. Lyman, and S. G. Purkey (2015), Informing deep argo array design using argo and full-depth hydrographic section data, *J. Atmos. Oceanic Technol.*, *32*(11), 2187–2198.
Johnson, G. C., J. M. Lyman, and N. G. Loeb (2016), Improving estimates of Earth's energy imbalance, *Nat. Clim. Change*, *6*(7), 639–640.
Levitus, S., J. Antonov, and T. Boyer (2005), Warming of the world ocean, 1955–2003, *Geophys. Res. Lett.*, *32*, L02604, doi:10.1029/2004GL021592.
Levitus, S., et al. (2012), World ocean heat content and thermosteric sea level change (0–2000 m), 1955–2010, *Geophys. Res. Lett.*, *39*, L10603, doi:10.1029/2012GL051106.
Locarnini, R., et al. (2013), *World Ocean Atlas 2013, Volume 1: Temperature*, S. Levitus, Ed., A. Mishonov Technical Ed.; NOAA Atlas NESDIS 73, 40 pp., Silver Spring, Md.
Loeb, N. G., B. A. Wielicki, W. Su, K. Loukachine, W. Sun, T. Wong, K. J. Priestley, G. Matthews, W. F. Miller, and R. Davies (2007), Multi-instrument comparison of top-of-atmosphere reflected solar radiation, *J. Clim.*, *20*(3), 575–591.
Loeb, N. G., B. A. Wielicki, D. R. Doelling, G. L. Smith, D. F. Keyes, S. Kato, N. Manalo-Smith, and T. Wong (2009), Toward optimal closure of the Earth's top-of-atmosphere radiation budget, *J. Clim.*, *22*(3), 748–766.
Loeb, N. G., J. M. Lyman, G. C. Johnson, R. P. Allan, D. R. Doelling, T. Wong, B. J. Soden, and G. L. Stephens (2012), Observed changes in top-of-the-atmosphere radiation and upper-ocean heating consistent within uncertainty, *Nat. Geosci.*, *5*(2), 110–113.
Lyman, J. M., and G. C. Johnson (2008), Estimating annual global upper-ocean heat content anomalies despite irregular in situ ocean sampling, *J. Clim.*, *21*(21), 5629–641.
Lyman, J. M., and G. C. Johnson (2014), Estimating global ocean heat content changes in the upper 1800 m since 1950 and the influence of climatology choice, *J. Clim.*, *27*(5), 1945–1957.
Lyman, J. M., S. A. Good, V. V. Gouretski, M. Ishii, G. C. Johnson, M. D. Palmer, D. M. Smith, and J. K. Willis (2010), Robust warming of the global upper ocean, *Nature*, *465*(7296), 334–337.
Palmer, M., K. Haines, S. Tett, and T. Ansell (2007), Isolating the signal of ocean global warming, *Geophys. Res. Lett.*, *34*, L23610, doi:10.1029/2007GL031712.
Robinson, D. A., K. F. Dewey, and R. R. Heim Jr. (1993), Global snow cover monitoring: An update, *Bull. Am. Meteorol. Soc.*, *74*(9), 1689–1696.
Roemmich, D., and J. Gilson (2009), The 2004–2008 mean and annual cycle of temperature, salinity, and steric height in the global ocean from the Argo Program, *Prog. Oceanogr.*, *82*(2), 81–100.
Roemmich, D., J. Church, J. Gilson, D. Monselesan, P. Sutton, and S. Wijffels (2015), Unabated planetary warming and its ocean structure since 2006, *Nat. Clim. Change*, *5*(3), 240–245.
Rohde, R., R. A. Muller, R. Jacobsen, E. Muller, S. Perlmutter, A. Rosenfeld, J. Wurtele, D. Groom, and C. Wickham (2013), A new estimate of the average Earth surface land temperature spanning 1753 to 2011, *Geoinfor. Geostat.*, *1*, 1.
Roquet, F., et al. (2013), Estimates of the Southern Ocean general circulation improved by animal-borne instruments, *Geophys. Res. Lett.*, *40*, 6176–6180, doi:10.1002/2013GL058304.
Smith, D. M., R. P. Allan, A. C. Coward, R. Eade, P. Hyder, C. Liu, N. G. Loeb, M. D. Palmer, C. D. Roberts, and A. A. Scaife (2015), Earth's energy imbalance since 1960 in observations and CMIP5 models, *Geophys. Res. Lett.*, *42*, 1205–1213, doi:10.1002/2014GL062669.
Toole, J. M., R. A. Krishfield, M.-L. Timmermans, and A. Proshutinsky (2011), The ice-tethered profiler: Argo of the Arctic, *Oceanography*, *24*(3), 126–135.
Trenberth, K. E. (2009), An imperative for climate change planning: Tracking Earth's global energy, *Curr. Opin. Environ. Sustainability*, *1*(1), 19–27.
Trenberth, K. E., J. M. Caron, and D. P. Stepaniak (2001), The atmospheric energy budget and implications for surface fluxes and ocean heat transports, *Clim. Dyn.*, *17*(4), 259–276.
Trenberth, K. E., J. T. Fasullo, K. von Schuckmann, and L. Cheng (2016), Insights into earth's energy imbalance from multiple sources, *J. Clim.*, *29*, 7495–7505, doi:10.1175/JCLI-D-16-0339.1.
von Schuckmann, K., and P.-Y. L. Traon (2011), How well can we derive Global Ocean Indicators from Argo data?, *Ocean Sci.*, *7*(6), 783–791.
von Schuckmann, K., J.-B. Sallée, D. Chambers, P.-Y. Le Traon, C. Cabanes, F. Gaillard, S. Speich, and M. Hamon (2013), Monitoring ocean heat content from the current generation of global ocean observing systems, *Ocean Sci. Discuss.*, *10*, 923–949.
von Schuckmann, K., J.-B. Sallée, D. Chambers, P.-Y. Le Traon, C. Cabanes, F. Gaillard, S. Speich, and M. Hamon (2014), Consistency of the current global ocean observing systems from an Argo perspective, *Ocean Sci.*, *10*, 547–557.
von Schuckmann, K., et al. (2016), An imperative to monitor Earth's energy imbalance, *Nat. Clim. Change*, *6*(2), 138–144.
Wielicki, B. A., B. R. Barkstrom, E. F. Harrison, R. B. Lee III, G. Louis Smith, and J. E. Cooper (1996), Clouds and the Earth's Radiant Energy System (CERES): An earth observing system experiment, *Bull. Am. Meteorol. Soc.*, *77*(5), 853–868.
Wijffels, S., D. Roemmich, D. Monselesan, J. Church, and J. Gilson (2016), Ocean temperatures chronicle the ongoing warming of Earth, *Nat. Clim. Change*, *6*(2), 116–118.
Wild, M., D. Folini, M. Z. Hakuba, C. Schär, S. I. Seneviratne, S. Kato, D. Rutan, C. Ammann, E. F. Wood, and G. König-Langlo (2015), The energy balance over land and oceans: An assessment based on direct observations and CMIP5 climate models, *Clim. Dyn.*, *44*(11–12), 3393–3429.
Willis, J. K., D. Roemmich, and B. Cornuelle (2004), Interannual variability in upper ocean heat content, temperature, and thermosteric expansion on global scales, *J. Geophys. Res.*, *109*, C12036, doi:10.1029/2003JC002260.

Willmott, C. J., C. M. Rowe, and Y. Mintz (1985), Climatology of the terrestrial seasonal water cycle, *J. Climatol.*, *5*(6), 589–606.
Worby, A. P., C. A. Geiger, M. J. Paget, M. L. Van Woert, S. F. Ackley, and T. L. DeLiberty (2008), Thickness distribution of Antarctic sea ice, *J. Geophys. Res.*, *113*, C05S92, doi:10.1029/2007JC004254.
Wunsch, C. (2016), Global ocean integrals and means, with trend implications, *Annu. Rev. Mar. Sci.*, *8*, 1–33.
Wunsch, C., and P. Heimbach (2013), Dynamically and kinematically consistent global ocean circulation and ice state estimates, in *Ocean Circulation and Climate: A 21 Century Perspective*, edited by G. Siedler et al., pp. 553–579, Academic Press, Oxford, U. K.
Zhang, J., and D. Rothrock (2003), Modeling global sea ice with a thickness and enthalpy distribution model in generalized curvilinear coordinates, *Mon. Weather Rev.*, *131*(5), 845–861.
Zuo, H., M. A. Balmaseda, and K. Mogensen (2015), The new eddy-permitting ORAP5 ocean reanalysis: Description, evaluation and uncertainties in climate signals, *Clim. Dyn.*,1–21, doi:10.1007/s00382-015-2675-1.